

The NIH MRI study of normal brain development[☆]

Brain Development Cooperative Group¹
Alan C. Evans*

Montreal Neurological Institute, McGill University, Department of Neurology and Neurosurgery, 3801 University St., Montreal, H3A 2B4 Canada

Received 28 January 2005; revised 8 July 2005; accepted 14 September 2005
Available online 11 January 2006

MRI is increasingly used to study normal and abnormal brain development, but we lack a clear understanding of “normal”. Previous studies have been limited by small samples, narrow age ranges and few behavioral measures. This multi-center project conducted epidemiologically based recruitment of a large, demographically balanced sample across a wide age range, using strict exclusion factors and comprehensive clinical/behavioral measures.

A mixed cross-sectional and longitudinal design was used to create a MRI/clinical/behavioral database from approximately 500 children aged 7 days to 18 years to be shared with researchers and the clinical medicine community. Using a uniform acquisition protocol, data were collected at six Pediatric Study Centers and consolidated at a Data Coordinating Center. All data were transferred via a web-network into a MYSQL database that allowed (i) secure data transfer, (ii) automated MRI segmentation, (iii) correlation of neuroanatomical and clinical/behavioral variables as 3D statistical maps and (iv) remote interrogation and 3D viewing of database content.

A population-based epidemiologic sampling strategy minimizes bias and enhances generalizability of the results. Target accrual tables reflect the demographics of the U.S. population (2000 Census data). Enrolled subjects underwent a standardized protocol to characterize neurobehavioral and pubertal status. All subjects underwent multi-spectral structural MRI. In a subset, we acquired T1/T2 relaxometry, diffusion tensor imaging, single-voxel proton spectroscopy and spectroscopic imaging. In the first of three cycles, successful structural MRI data were acquired in 392 subjects aged 4:6–18:3 years and in 72 subjects aged 7 days to 4:6 years. We describe the methodologies of MRI data acquisition and analysis, using illustrative results.

This database will provide a basis for characterizing healthy brain maturation in relationship to behavior and serve as a source of control data for studies of childhood disorders. All data described here will be available to the scientific community from July, 2006.

© 2005 Elsevier Inc. All rights reserved.

Keywords: Pediatric; MRI; Database; Brain behavior; Multi-center

[☆] Researchers who are interested in using the database resulting from this project are encouraged to request the protocols by e-mailing rozie@bic.mni.mcgill.ca.

* Corresponding author. Fax: +1 514 398 8948.

E-mail address: alan.evans@mcgill.ca (A.C. Evans).

¹ See Appendix A for author list.

Available online on ScienceDirect (www.sciencedirect.com).

Introduction

Magnetic resonance imaging (MRI) has made it possible to study normal structural and metabolic brain development across age groups. It had been difficult to study infants, children and adolescents with earlier imaging modalities because of safety concerns related to radiation exposure. Hence, relatively little was known about healthy brain development in humans prior to the advent of MRI.

Background

In the 1990s, several research groups demonstrating age-related changes in gray matter volumes, white matter volumes, myelination and subcortical measures with MRI in samples of healthy children aged 4–21 years (Filipek et al., 1994; Jernigan and Tallal, 1990; Jernigan et al., 1991; Pfefferbaum et al., 1994). Subsequently, additional studies have described normal developmental changes in specific brain regions based on samples of children and young adults ranging in size from $N = 13$ to 176 (Bartzokis et al., 2001; Blanton et al., 2001, 2004; Blatter et al., 1995; Caviness et al., 1996, 1999; Courchesne et al., 2000; DeBellis et al., 2001; Giedd et al., 1996, 1999; Gogtay et al., 2002, 2004; Kennedy et al., 1998, 2003; Lange et al., 1997; Paus et al., 1999; Reiss et al., 1996; Sowell et al., 1999, 2002, 2003, 2004a). Several recent reviews have summarized this research (Durstun et al., 2001; Gogtay et al., 2002; Paus et al., 2001; Sowell et al., 2004b) with respect to maturation and correlation with postmortem findings in infancy and childhood. It is clear that during early childhood and adolescence specific regional brain measures vary widely in healthy populations. Cross-sectional studies have therefore been limited in the conclusions they can reach about healthy brain development. Similarly, studies of pediatric brain disorders have been hampered by the lack of control data for healthy development. Longitudinal studies have noted that individual developmental brain growth trajectories are highly variable, regionally specific and may demonstrate gender-specific patterns (Giedd et al., 1996, 1999). They highlight the need for large sample sizes in order to obtain reliable conclusions about the normative range for specific regional volumetric data and maturation patterns (Gogtay et al., 2004).

Although a few studies have demonstrated relationships between healthy regional brain structure maturation and specific cognitive abilities, this area of research remains largely untapped (Casey et al., 1997; Sowell et al., 2004b). Significant questions regarding healthy brain development remain. Previously reported studies of self-selected samples, obtained through a variety of media solicitations or samples of convenience, are not representative of U.S. demographics, particularly with respect to race, ethnicity and income. Thus, the generalizability of reported results is limited. Little data have been reported on children younger than age six, a population of particular interest because of rapid brain development during infancy and preschool years. Very few longitudinal studies have been conducted. Most have been limited to analysis of T1-weighted data only. The absence of cross-site collaborations or image acquisition standardization further limits our understanding of brain development and brain–behavior relationships and limits the generalizability or useful application of control data across research laboratories. As yet, no representative, longitudinally acquired database of healthy brain development that combines high quality multi-sequence, multi-modality MR images: anatomical MRI (aMRI), magnetic resonance spectroscopy (MRS) and diffusion tensor imaging (DTI) with comprehensive longitudinal clinical/neurobehavioral assessments is available.

One example of the impact of this knowledge gap can be seen in a recent report of differences in brain morphology between children with attention deficit hyperactivity disorder (ADHD) and healthy controls (Castellanos et al., 2002). This study reported subtle, yet widespread, reductions in regional brain volumes that were generally stable across development with the exception of early reductions in caudate volume which appeared to normalize during adolescence. Despite its utilization of one of the largest normal MRI data sets available (Giedd et al., 1999), this study was limited by a paucity of data for the younger ages, where reliable predictions were not possible. Fewer than 20 healthy male and 10 healthy female children were under 8 years of age in that study. Furthermore, the control data set had restricted socioeconomic representation and (high) IQ range (elevated relative to the ADHD sample). A more complete and representative database of MRI and cognitive/behavioral measures in a demographically diverse sample will greatly increase the power for detecting subtle, yet important, differences in brain developmental trajectories in childhood psychiatric and neurological disorders.

Present study

This study was undertaken in order to establish a public database of pediatric aMRI, MRS and DTI brain scans, for several purposes: (1) to elucidate healthy anatomic and metabolic brain development, providing ranges of normal values and defining key developmental periods; (2) to fill a need for a representative and reliable source of healthy control subject data for studies of childhood disorders and brain diseases to be made available to pediatric researchers and clinicians; (3) to provide data for the construction of healthy developmental growth curves for specific brain structures and metabolites; and (4) to aid the development of image analysis methods and diagnostic tools, e.g., the derivation of developmentally sensitive morphometric or metabolic imaging measures not obtainable with methods developed for adult populations.

A major goal was to recruit a demographically representative healthy sample. In order to meet this goal and to minimize ascertainment biases that can be present in samples of convenience, a population-based sampling method was employed. A sample of healthy infants, children and adolescents demographically representative of the U.S. population has been recruited and characterized. Cognitive, neuropsychological and behavioral measures were acquired to screen or exclude subjects as well as to provide a basis for brain–behavior correlational studies with the imaging data.

Collecting neuroanatomical and clinical/behavioral data from children ranging in age from 7 days to 18:3 years is challenging due to the impracticality of applying a common data acquisition protocol across these ages. Many clinical/behavioral measures are only suitable for a limited age range. Similarly, for MR imaging, the optimal scanning protocol depends upon tissue characteristics and practical considerations which vary with age (subject tolerance, motion). Accordingly, the primary goal of the project, the collection of structural MRI and behavior data, was organized as two “Objectives”. The larger Objective 1 includes children in the age range of 4:6–18:3 years, while the smaller Objective 2 includes children from 7 days to 4:6 years. Although the underlying goals of these Objectives are similar, the protocols for recruitment, screening, behavioral and cognitive characterization, MR scanning and sampling frequency differ substantially. Both Objectives employ a longitudinal study design: Objective 1 children are being scanned at 2-year intervals while Objective 2 children are being scanned at approximately quarterly intervals (Figs. 1, 2).

A comprehensive description of each component of this multifaceted project within a single report would be prohibitively long. Nevertheless, an accurate representation of the overall project context requires that all elements be presented together. This report therefore outlines the overarching rationale and methodologies of the project, with emphasis on Objective 1. Subsequent reports will provide greater detail regarding other individual components (e.g., Objective 2, MRS, DTI) and their results.

Thus far, the project has enrolled a cohort of 433 Objective 1 subjects and 72 Objective 2 subjects and is following these subjects over a 7-year period. Data are collected at six pediatric study centers (PSCs):

Boston—Children’s Hospital
Cincinnati—Children’s Hospital Medical Center
Houston—University of Texas Houston Medical School
Los Angeles—Neuropsychiatric Institute and Hospital, UCLA
Philadelphia—Children’s Hospital of Philadelphia (CHOP)
St. Louis—Washington University.

Informed consent from parents and adult subjects and child assents were obtained for all subjects enrolled at the PSCs. All protocols and procedures were approved by the relevant Institutional Review Board at each PSC and at each coordinating center.

A Clinical Coordinating Center (CCC) at Washington University St. Louis coordinates the clinical/behavioral aspects of the project including: sampling plan and methods; subject recruitment, inclusion/exclusion criteria and screening/assessment protocols; quality control (QC) for the administration of all clinical and behavioral measures. Structural MRI and clinical/behavioral data

are consolidated and analyzed within a purpose-built database at a Data Coordinating Center (DCC) at the Montreal Neurological Institute, McGill University. The DCC coordinates the image acquisition protocols, imaging data quality control and image analysis. Diffusion tensor imaging (DTI) data are analyzed at a DTI Processing Center, National Institute of Child Health and Development (NICHD) NIH (DPC). Spectroscopy data are analyzed at a Spectroscopy Processing Center UCLA (SPC). All data, raw and processed, are eventually consolidated at the DCC.

Three separate repeated study cycles for each child allow both longitudinal and cross-sectional analysis. Imaging and clinical/behavioral data are transferred via a web-based network into a central database that allows for (i) secure, encrypted data transfer and automated quality control, (ii) automated large-scale MRI segmentation, (iii) correlation of neuroanatomical and clinical/behavioral variables as 3D statistical maps and (iv) remote interrogation and 3D viewing of database content.

Imaging data included structural MRI (T1-weighted, T2-weighted, proton-density-weighted). A subset of children had additional data acquisitions (T1/T2 relaxometry, DTI, MRS and MRS imaging (MRSI)). In the following sections, we describe the methodologies for sampling and recruitment, clinical and behavioral assessment, MRI data acquisition, database design, MR segmentation and Data analysis.

Methods

Sampling and recruitment

Population-based sampling

The population-based sampling method used in this study seeks to minimize biases that can be present in samples of convenience in order to maximize the generalizability of the data collected. The sampling plan for each PSC was developed from the available Census 2000 data, which allowed neighborhood demographic variables to be estimated for the corresponding zip codes (so called geocoding). This allowed targeted recruitment and comparison to the general population by reference to geocoded census data. Geocoding further allowed for estimation of demographic information on subjects who decline or were excluded from participation. Recruitment was monitored continuously by the CCC in order to assure that the sample recruited across all PSCs was demographically representative. Regional PSC-specific enrollment targets were employed until approximately 50% of the sample was accrued, at which time the remaining targeted subjects were recruited collectively by all sites. Once specific demographic target goals were reached, those enrollment “cells” were closed.

Recruitment and screening procedures. Names and addresses for households with children in the age range of interest were obtained from a marketing agency (Info U.S.A.). Recruitment and screening proceeded in a multi-stage process, including mailing introductory letters followed by a brief screening phone interview, parental completion of a Childhood Behavior Checklist for the child of interest (CBCL, Achenbach, 2001; Achenbach and Rescorla, 2000) (exclusion a T score ≥ 70 on any clinical subscale).

For those who passed the brief screener, a longer phone “full screening interview” included more detailed health and neurological history and inquiries about most exclusion criteria (see Table

1). If no exclusion criteria were met, this screening interview was passed, the Diagnostic Interview Schedule for Children (C-DISC-4, Shaffer et al., 2000), a structured psychiatric interview, was completed with the parent about the child. Children 11 years of age and older also completed the Diagnostic Predictive Scales (DPS, Lucas et al., 2001) about themselves. If the DPS interview indicated possible diagnoses, it was followed-up with the C-DISC-4 administered to the adolescent (Shaffer et al., 2000). Parents also completed a semi-structured interview covering first-degree family history of psychiatric disorders—the Family Interview for Genetic Studies (FIGS, Initiative NSaBDG, 1992 [MRI modified version, FIGS-MRI]). Families and children who passed screening were invited in for the full-day protocol.

Males and females and right- and left-handed individuals were included. Exclusion criteria included factors which are established or highly suspected to adversely impact healthy brain development or to prohibit completion of the full study protocol, e.g., contraindications for MRI scanning. In uncertain cases, an internal panel, comprised of a subset of the investigators, reviewed relevant data and made the include/exclude decision by simple majority.

Clinical and behavioral assessment

An important aspect of this study is the investigation of correlation between (a) performance on cognitive and behavioral tasks and (b) measures of brain structure and function across development, e.g., between: (1) hand preference and cerebral asymmetries, (2) executive functions assessed with the Cambridge Neuropsychological Test Automated Battery (CANTAB, CeNeS Limited, 1999) and frontal cortical structural features (Luciana, 2003; Luciana and Nelson, 2002; Robbins et al., 1998) and (3) motor dexterity based on Purdue Pegboard (Gardner and Broman, 1979) scores and specific motor cortex volumes or corticospinal white matter densities.

A battery of tests and inventories were selected to assess basic cognitive and behavioral skills over the age range of interest. Preference was given to well standardized, clinically interpretable tests with well-established psychometric properties. Neurological and other behavioral measures, such as those reflecting temperament, personality or behavioral styles, were chosen to be quantitative and capable of capturing normal healthy developmental variability. Since all components of the study were to be completed typically in one all-day visit, the test battery had to be completed within 2 to 3 h (including breaks) for children of all ages. The test battery, listed in Table 2, samples a wide range of functions/abilities from fine motor skills through higher levels of perceptual and cognitive processing. The measures used change over the wide age range of Objective 1 subjects (4: 6–18: 3 years). Some tests were potentially exclusionary, while others were included for sample characterization and brain–behavior correlation. A pediatric physical (including neurological) examination was used to detect neurological abnormalities for exclusionary purposes, as well as to provide data for correlation with other neurobehavioral and neuroimaging data.

The collection of both physical data from a self-rating Tanner scale (Carskadon and Acebo, 1993; Peterson et al., 1988) and endocrine data (from saliva and urine samples) provided a more complete physiologic profile to correlate with neuroimaging data. Tanner staging (e.g., Tanner, 1962) will be used to discern the effect(s) of physiologic pubertal changes on brain structure and biochemistry. Children also provided two separate 1–3 cm³

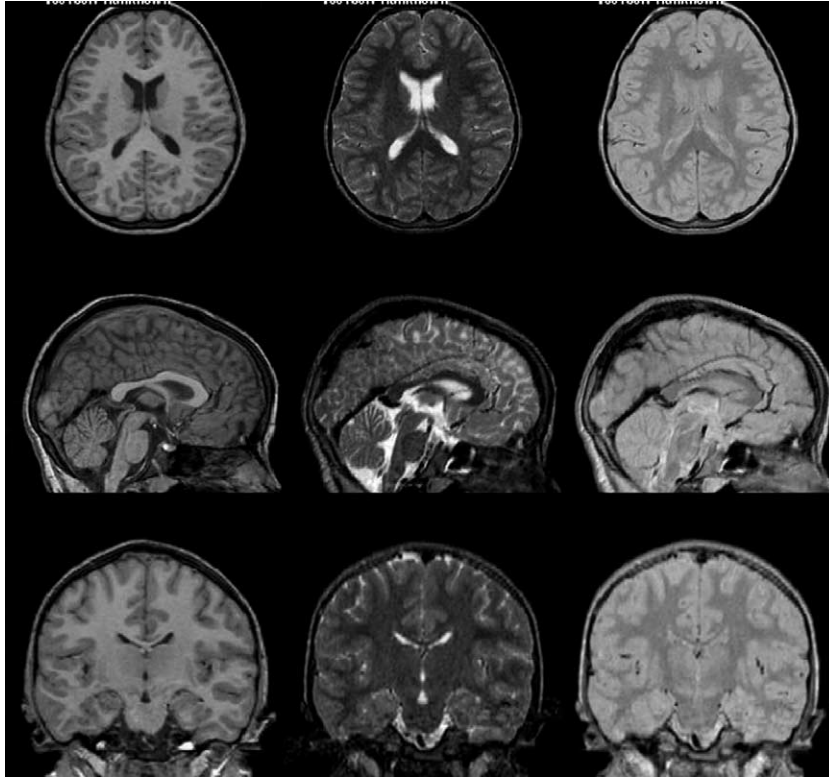


Fig. 1. Objective 1 sample data (T1W/T2W/PDW).

samples of saliva and a urine sample which will both be assayed by published radioimmunoassays (RIA) methods for testosterone (male subjects) and estradiol (females) at one PSC (UCLA).

Quality control measures for screening, neurological and behavior evaluations

Quality control (QC) procedures were implemented by the CCC to monitor the administration of all neurobehavioral tests and inter-

views to assure the uniform application of recruitment procedures and assessment protocols across PSCs. Details are available on the project website (<http://www.bic.mni.mcgill.ca/nihpd/info>).

MR data acquisition

MRI scanners used were 1.5 T systems from General Electric (GE) or Siemens Medical Systems (Siemens).

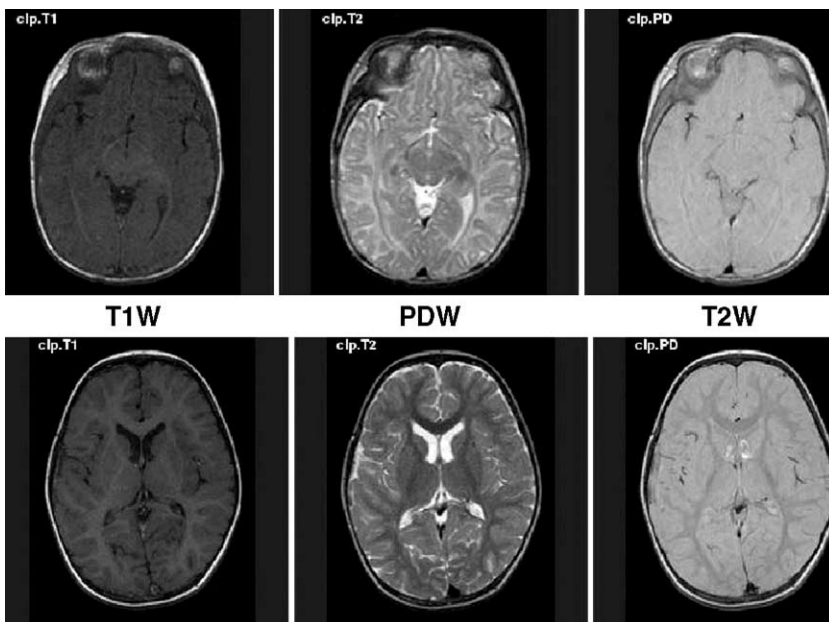


Fig. 2. Objective 2 MRI sample images: Top—3 months; bottom—30 months.

Table 1
Exclusion criteria

Demographic	Children of parents with limited English proficiency. Adopted children excluded due to inadequate family histories
Pregnancy, birth and perinatal history	Intra-uterine exposures to substances known or highly suspected to alter brain structure or function (certain medications, any illicit drug use, smoking >1/2 pack per day or >2 alcoholic drinks per week during pregnancy) Hyperbilirubinemia requiring transfusion and/or phototherapy (>2 days); gestational age at birth of <37 weeks or >42 weeks; multiple birth; delivery by high forceps or vacuum extraction; infant resuscitation by chest compression or intubation; maternal metabolic conditions, e.g., phenylketonuria; diabetes; preeclampsia; serious obstetric complication; general anesthesia during pregnancy/delivery; C-section for maternal or infant distress
Physical/medical or growth	Current height or weight <3rd percentile; head circumference <3rd percentile; by National Center for Health Statistics 2000 data (charts at http://www.cdc.gov/nchs/about/major/nhanes/growthcharts/charts.htm ; Nellhaus, 1968). History of significant medical or neurological disorder with CNS implications (e.g., seizure disorder, CNS infection, malignancy, diabetes, systemic rheumatologic illness, muscular dystrophy, migraine or cluster headaches, sickle cell anemia, etc.); history of closed head injury with loss of consciousness >30 min or with known diagnostic imaging study abnormalities; systemic malignancy requiring chemotherapy or CNS radiotherapy; hearing impairment requiring intervention; significant visual impairment requiring more than conventional glasses; (strabismus, visual handicap); metal implants (braces, pins) if likely to pose safety or artifact issues for MRI; positive pregnancy test in subject
Behavioral/psychiatric	Current or past treatment for language disorder (simple articulation disorders not exclusionary); a lifetime history of Axis I psychiatric disorder (except for simple phobia, social phobia, adjustment disorder, oppositional defiant disorder, enuresis, encopresis, nicotine dependency); any CBCL subscale score ≥ 70 ; WASI IQ <70; Woodcock–Johnson III Achievement Battery subtest score <70; current or past treatment for an Axis I psychiatric disorder
Family history	History of inherited neurological disorder; history of mental retardation due to non-traumatic events in any first-degree relative; one or more first-degree relatives with lifetime history of Axis I psychiatric disorders: schizophrenia, bipolar affective disorder, psychotic disorder, alcohol or other drug dependence, obsessive compulsive disorder, Tourette's disorder, major depression, attention deficit hyperactivity disorder or pervasive developmental disorder
Neuro examination	Abnormality on neurological examination, e.g., hypertonia, hypotonia, reflex asymmetry, visual field cut, nystagmus and tics

MRI protocol for Objective 1

Objective 1 uses MRI for the *in vivo* characterization of developing brain structure in children aged 4.6–18.3 years. In order to collect data within the time limitations for this age range and allow automated morphometric analysis, 30–45 min of data acquisition was allocated, with 1 mm in-plane resolution, 1–2 mm slice thickness, whole brain coverage and multiple contrasts (T1W, T2W and PDW).

We selected a 3D T1-weighted (T1W) spoiled gradient recalled (SPGR) echo sequence (see Table 3). The primary alternative considered was a 3D magnetization prepared gradient echo sequence (3D MPRAGE); however, following extensive multi-center testing with multiple MRI vendors, the conventional 3D SPGR was found to provide a higher signal-to-noise/contrast-to-noise ratios and more consistent results. The protocol provides 1 mm isotropic data from the entire head. As the priority measure for Objective 1, it was acquired immediately following the localizer scan and, if significant motion artifacts were observed, was immediately repeated. On GE scanners, the maximum number of slices was 124, and hence the slice thickness was increased (~1.5 mm) to give whole head coverage. Sagittal acquisition was chosen, being the most efficient way to obtain complete head coverage.

A dual contrast, proton density- and T2-weighted (PDW and T2W) acquisition provided additional information for automated multi-spectral tissue classification/segmentation. An optimized 2D multislice (2 mm) dual echo fast spin echo (FSE) sequence was used. An oblique axial orientation (parallel to the AC–PC line)

was selected, both for potential use of the data within a radiological atlas and for consistency between Objectives 1 and 2.

Not all Objective 1 subjects, particularly the youngest, could tolerate the optimal scanning protocol described above (a ~15-min 3D T1W and ~10-min PDW/T2W scan). In anticipation of this problem, we implemented a fall-back MR protocol that consisted of shorter 2D acquisitions which provides acceptable structural images and continuity with the Objective 2 MR protocol.

A 2D T1W multislice (MS) spin echo (SE) was substituted when motion degraded the 3D T1W scan. Data were collected parallel to the AC–PC line with a $1 \times 1 \times 3$ mm spatial resolution. If the PDW/T2W scan was degraded by motion, slice thickness was increased from 2 mm to 3 mm, reducing scan time and likelihood of motion.

MRI protocol for Objective 2

Because brain development early in life is rapid, MR relaxation rates vary dramatically. Furthermore, the movement problems which occur when scanning very young children dictate short acquisitions. This fast, robust protocol provides data similar to Objective 1, as well as quantitative relaxation data.

The principal component acquires data similar to Objective 1, for image segmentation. A 3D T1W 1 mm isotropic acquisition is unrealistically long for this age group, so a 2D T1W multislice spin echo was a practical compromise. Data were collected parallel to the AC–PC line with a $1 \times 1 \times 3$ mm spatial resolution. The parameters of this sequence are identical to the Objective 1 fall-

Table 2
Subject and parent procedures for Objective 1

Instrument/procedure		For	Age range
Childhood Behavior Checklist (CBCL) (Achenbach, 1997; Achenbach and Rescorla, 2000; Achenbach, 2001)	CBCL/1:5–5	Parent	4:6 to 5:11 years
	CBCL/6–18	Parent	6:0 to 17:11 years
	Young Adult Self-Report (YASR)	Subject	>18 years
Brief Telephone screening interview		Parent	All
Full telephone screening interview		Parent	All
Diagnostic Interview Schedule for Children (C-DISC-4) (Shaffer et al., 2003)		Parent	>7 years
DISC Predictive Scales (DPS-4) (Lucas, 2003). If positive, C-DISC-4 (Shaffer et al., 2000)		Subject	>11 years
Family history Interview for Genetic Studies (FIGS-MRI, Initiative NsaBDG, 1992)		Subject	All
Behavior Rating Inventory of Executive Function (BRIEF) (Gioia et al., 1996, 2000)		Parent	All
Junior Temperament Character Inventory and Temperament Character Inventory (JTCI, TCI, Cloninger et al., 1993, 1994; Constantino et al. (2002)	Parent JTCI	Parent	4:6 to 14:11 years
	Child JTCI	Subject	10:0 to 14:11 years
	Young Adult TCI	Subject/Parent	>15 years
Physical/neurological examination		Subject	All
Tanner Staging Questionnaire (Peterson et al., 1988)		Subject	Examiner discretion
Urine sampling for testosterone and estradiol		Subject	All
Pregnancy screening test		Subject	All menstruating females
Saliva sampling (collected 2 times) for cortisol		Subject	All
Handedness (Almli, 1999)		Subject	All
Differential Abilities Scale (DAS) (Elliott, 1990a,b,c)		Subject	4:6 to 5:11 years
Wechsler Abbreviated Scale of Intelligence (WASI, Wechsler, 1999)	Vocabulary	Subject	>6 years
	Similarities	Subject	
	Block Design	Subject	
	Matrix Reasoning	Subject	
Wechsler Intelligence Scale for Children (WISC-III, Wechsler, 1991)	Digit Span	Subject	4:6 to 16:11 years
	Coding	Subject	
Wechsler Adult Intelligence Scale-Revised (WAIS-R, Wechsler, 1981)	Digit span	Subject	>17 years
	Digit symbol	Subject	
Woodcock–Johnson-III (WJ-III) Letter–Word Identification, Passage Comprehension, Calculation (Woodcock et al., 2001)		Subject	All
California Verbal Learning Test (CVLT) (Delis et al., 1994, 2000)	CVLT-C	Subject	4:6 to 15:11 years
	CVLT-II	Subject	>16 years
NEPSY (Korkman et al., 1998)	Verbal Fluency	Subject	All
	Semantic Category	Subject	>12 years
Purdue Pegboard (Gardner and Broman, 1979)	Half Board	Subject	4:6 to 11:11 years
	Full Board	Subject	>6 years
Cambridge Neuropsychological Test Automated Battery (CANTAB) CeNeS Ltd (1999)		Subject	All

back T1W scan (see Table 4). The sequence took less than 5 min and was repeated if degraded by motion artifacts.

The second component acquired PDW/T2W data with the same orientation and spatial resolution as the T1W data. The sequence type (dual contrast FSE) and parameters were otherwise identical to those of the Objective 1 fall-back PDW/T2W scan. The measurement also took <5 min and was repeated if corrupted by motion. While this approach provides PDW/T2W data consistent with Objective 1, a stronger T2 weighting is preferable for very young infants who have longer T2 relaxation times, so a second dual contrast FSE sequence with heavier T2 weighting was added.

The final component acquired quantitative relaxometry. For T1 relaxometry, an inversion recovery sequence developed by Haselgrove et al. (2000) was adopted. Acquisitions were in the oblique axial plane with a slice thickness of 3 mm. In-plane resolution was 2 mm as dictated by single shot (EPI or SSFSE/HASTE) readout. Good quality multi-component T2 relaxometry

could only be performed one slice at a time using 32 or more echoes and at least 6 min/slice. Such data provide important information regarding myelination, but the duration prevents its use over the entire brain. We used dual (effective) echo FSE data to estimate T2 for a single compartment model (Table 5).

Magnetic resonance spectroscopy (MRS) protocol

Intermediate-TE single-voxel MRS. Single-voxel in vivo proton MRS data were acquired at 1.5 T in Boston (Obj. 1 and 2), CHOP (Obj. 1) and UCLA (Obj. 1). Due to the limited SNR of proton MRS and extra time required for shimming, only single-voxel MRS acquisitions were performed at the initial visit. An intermediate echo time PRESS acquisition, with voxels measuring $15 \times 15 \times 15$ mm (3.375 cm³), and 64 signal averages produced acceptable SNR spectra in a scan time of ~3 min per voxel (see Table 6). Four voxels of interest corresponded to the left frontal and parietal white matter, left thalamus and right occipital gray matter. For GE machines, 8 averages of non-water-suppressed

Table 3
Objective 1 MRI acquisition details

	3D T1-weighted	2D PD/T2-weighted
Sequence	3D RF-spoiled gradient echo	Fast/Turbo spin echo (ETL/Turbo factor 8)
TR (ms)	22–25	3500
TE (ms)	10–11	
Excitation pulse	30°	90°
Signal averages	1	1
TE1 (effective) (ms)		15–17
TE2 (effective) (ms)		5–119
Refocusing pulse	180°	180°
Orientation	Sagittal	Oblique axial (AC–PC)
Thickness, gap (mm)	1, 0	2, 0
# of slices	Ear to ear	Apex to below cerebellum
Field of view (mm)	AP: 256 LR: 160–180 (whole head)	AP: 256 LR: 224
Matrix (mm)	AP: 256 LR: for 1 mm isotropic	AP: 256 LR: 224
Scan time (min)	15–18 (depends on head size)	7–11 (depends on head size)

MRS were automatically acquired under the PROBE procedure; for Siemens scanners, non-water-suppressed MRS (NEX = 8, otherwise identical) was acquired in the same voxel. Data processing was performed at the Spectroscopy Processing Center (SPC) at UCLA (see below).

Short-TE MRS imaging (MRSI). Proton MRS imaging (MRSI) was impractical within a single MR session, particularly for Objective 2. Two sites (UCLA and CHOP) undertook separate MRSI studies (1.5 T Siemens Sonata, standard quadrature head coil).

Table 4
Objective 1 fall-back MRI protocol

	T1-weighted	2D PD/T2-weighted
Sequence	Spin echo	Fast/Turbo spin echo (ETL/Turbo factor 8)
TR (ms)	500	3500
TE (ms)	12	
Flip angle	90°	90°
Signal averages	1	1
TE1 (effective) (ms)		15–17
TE2 (effective) (ms)		5–119
Refocusing pulse	180°	180°
Orientation	Oblique axial (AC–PC)	Oblique axial (AC–PC)
Thickness, gap (mm)	3, 0	3, 0
# of slices	Apex to below cerebellum	Apex to below cerebellum
Field of view (mm)	AP: 256 LR: 192	AP: 256 LR: 192
Matrix	AP: 256 LR: 192	AP: 256 LR: 192
Scan time (min)	3–5 (depends on head size)	4–7 (depends on head size)

Table 5
Objective 2 protocol for relaxometry

	Quantitative T1	Dual contrast T2W
Sequence	IR-prepared single-shot EPI or single-shot Fast/Turbo spin echo	Fast/Turbo spin echo (ETL/Turbo factor 8)
TR (ms)		3300
Signal averages	1	1
TE1 (effective) (ms)		83
TE2 (effective) (ms)		165
Refocusing pulse		180°
Orientation	Oblique axial (AC–PC)	Oblique axial (AC–PC)
Thickness, gap (mm)	3, 0	3, 0
# of slices	Apex to below cerebellum	Apex to below cerebellum
Field of view (mm)	AP: 256 LR: 192	AP: 256 LR: 192
Matrix	AP: 128 LR: 96	AP: 256 LR: 192
Scan time (min)	10–12 (depends on head size)	3–5 (depends on head size)

UCLA. Three pairs of axial–oblique (A–O) MRSI data sets (2D PRESS, TR/TE = 1500/30 ms) were collected (Fig. 7). Each pair included water-suppressed (8 averages, ~11 min) and unsuppressed (1 average, ~4 min) acquisitions, the latter yielding a reference peak for absolute quantitation of MRSI metabolite levels and for eddy current correction. MRSI data were acquired as a 4×4 array of 1×1 cm² voxels within the following protocol:

- Scout-I (set-up ~1 min)
- Structural (A–O, double spin echo; TR/TE1/TE2 = 3500/17/119 ms; $1 \times 1 \times 3$ mm; ~4 min)
- Structural-I (sagittal 3D T1W; TR/TE = 25/11 ms; $1 \times 1 \times 1.2$ mm; ~10 min)
- MRSI-I anterior cingulate, prefrontal white (~15 min)
- Structural-II (repeat of 3D T1W to check for movement; ~10 min)
- Scout-II (bilateral frontal; $1 \times 1 \times 3$ mm; ~1 min)
- MRSI-II caudate, putamen, thalamus, insula, occipital gray (~15 min)
- DTI (~4 min)
- MRSI-III dorsolateral prefrontal gray (~15 min).

CHOP. Four MRSI slices parallel to the genu–splenial line and centered at the corpus callosum were selected as the ROI for

Table 6
Single-voxel MRS protocol

	Single voxel
Sequence	PRESS (customized to GE or Siemens)
TR (ms)	1500
TE (ms)	144
Flip angle	90°
Signal averages	64
Voxel size (mm)	$15 \times 15 \times 15$
White matter voxels	Left frontal, left parietal
Gray matter voxels	Left thalamus, midline occipital
Scan time (min)	6–20

optimal brain coverage. The MRSI box extended anteriorly to the genu of corpus callosum and posteriorly past the parahippocampal gyri. The top MRSI slab covered bilateral centrum semiovale regions. Three-plane HASTE localizer scans were acquired before each MRS/MRSI study. Oblique slices were used for optimal and reproducible slice positioning. Outer volume saturation was used to minimize lipid contamination from outside the ROI. Five to six 50 mm saturation bands were applied. Total scan time for HASTE localization, four single-voxel MRS scans and MRSI was ~23 min.

Typical parameters were:

- TR = 1300 ms, TE = 30 ms, 2 signal averages
- Rectangular ROI ($8 \times 8 \times 6$ cm typical), in-plane voxel $1 \times 1 \times 1$ cm³,
- Four 1.5 cm slices (FOV = $16 \times 16 \times 12$ cm),
- Scan resolutions = 16 (R/L) \times 16 (A/P) \times 8 (F/H),
- Data size = 1024 with a receiver bandwidth = 1200 Hz.
- Water suppression bandwidth = 50 Hz.

Diffusion tensor (DTI) protocol

This ancillary study collected diffusion tensor data from children aged from 7 days to 18 years. These data should provide specific information on white matter maturation and fiber orientation in the developing brain. DTI data were acquired at a subset of PSCs (Boston, Cincinnati, Philadelphia, St. Louis) with a diffusion-encoded multislice spin echo EPI sequence (see Table 7). To avoid orientation bias, data were acquired on a $3 \times 3 \times 3$ mm matrix covering the entire brain with straight axial slices (Fig. 3).

Overall acquisition priorities and ordering

For Objective 1, the most important acquisition was the T1W 3D volume scan. This was repeated if necessary and had to be successfully completed before proceeding to the PDW/T2W FSE. For Objective 2, the essential T1W and PDW/T2W acquisitions were repeated until satisfactorily acquired or the session aborted. They were followed by T1 relaxometry, DTI, MRS and the second dual contrast FSE.

Pediatric database

The database was designed to provide:

- Receipt and storage of all data (MRI and clinical/behavioral) acquired
- An intuitive interface reflecting the work and data flow
- Interfaces for clinical/behavioral data entry that mimic the ‘actual’ test forms
- Immediate, automatic QC of valid data entry, e.g., type, range; redundancy checks
- Facilities for ‘manual’ quality control at several stages
- Automatic data transfer (MRI and behavior) between PSCs and DCC
- Communication (bug-reporting, documentation, statistics) between PSCs and DCC
- Dissemination of data to wider scientific community under pre-defined access control.

Storage of MRI data was relatively straightforward with a limited number of large files per subject. The clinical/behavioral

Table 7
DTI protocol details

	Objective 1	Objective 2
Sequence	Diffusion encoded spin echo EPI (GE: custom, Siemens: EP2D_diff)	
TR (ms)	Minimum 3000 but 9000 for 60 slices	
TE (ms)	Minimum achievable with full echo acquisition	
Excitation angle	90°	
Signal averages	1	
<i>b</i> -values	0.1000	0.1000; 0.500
Diffusion directions	(1 0 1) (−1 0 1) (0 1 1) (0 1 −1) (1 1 0) (−1 1 0)	
# of series acquired	4	6
# of images/slice	$4 * (1 * b = 0 + 6 * b = 1000) = 28$	$4 * (1 * b = 0 + 6 * b = 1000) + 2 * (1 * b = 0 + 6 * b = 500) = 42$
Orientation	Straight axial	
Thickness, gap (mm)	3, 0	
# of slices	48–60 (from above apex to below cerebellum)	
Field of view (mm)	AP = 192, LR = 192 if head fits within 19 cm, else AP = 384, LR = 384	
Matrix	AP = 64, LR = 64 if head fits within 19 cm, else AP = 128, LR = 128	
Scan time (min)	4–7	

Parameters are the same for Objective 1 and 2 unless explicitly shown.

data were more complex, due to the wide range of data types. Numerous instruments included in the clinical/behavioral test battery are third party, commercial packages. These were configured on each PSC laptop by the DCC. Each test was implemented as a separate module with real-time scoring feedback during data entry.

Database architecture

The major components of the system (Fig. 4) are: (i) the PSC MRI scanner; (ii) a PC/Linux-based study workstation installed at each PSC, functioning as a data upload gateway to the DCC database; (iii) a laptop-based test administration system for clinical/behavioral tests (“laptop”); (iv) the database hardware and software at the DCC, allowing data entry and access through pre-defined access mechanisms; (v) the BIC image processing pipeline; (vi) a data backup system for the DCC database. The database uses MySQL, an Open Source Database Management System (<http://www.mysql.com>). MySQL is a database management system that incorporates a relational model for its databases and supports ANSI SQL (standard querying language). MySQL was chosen for its robustness, speed, reliability, free distribution and support. This architecture will support the public access to the database from July, 2006.

The database had to handle multi-site data acquisition and repeated testing of subjects during the study and to assure subject confidentiality. Task complexity was further increased due to the



Fig. 3. Diffusion-weighted images acquired according to DTI protocol in Table 7. The first image corresponds to $b = 0 \text{ s/mm}^2$. The six diffusion-weighted images that follow each represent one of the diffusion-encoding directions ($b = 1000 \text{ s/mm}^2$).

age-dependent protocol for clinical/behavioral measures and repeated MR procedures. The architecture employed three tiers to achieve this:

- Database Layer—a relational database (server side)
- Application Logic Layer—application logic controls user access and query execution
- Front-end Layer—web-based graphical user interface (GUI) (client side).

This enabled applications to be distributed over many physical locations and computing platforms. Clients accessed the database via front-end interfaces (e.g., GUIs) developed to best suit their computing environments. These interfaces can be implemented using virtually any programming language and even other database GUIs.

Database layer. The database core is a relational database with approximately 5000 fields per subject for (i) neurological, psychological, psychiatric and medical data (raw and derived scores) and (ii) MRI raw data, derived image volumes, morphological measures and MRI header data.

Application logic layer. The middle tier consists of user management functions which verify user accounts/access privileges. A series of PHP (server-side), Perl and Java scripts dynamically develop SQL to query the Database, receive and

process resulting data sets and present them to the front-end applications for display to the client.

Front-end layer. The front-end mirrors study workflow. Its main menus include:

1. Candidate Recruitment Stage/Menu—initial recruitment of a study candidate
2. Candidate Screening Stage/Menu—pre-visit screening of the candidate
3. Candidate Visit Stage/Menu—actual candidate's visit to the PSC
4. Approval Stage/Menu—post-visit evaluation of collected data
5. DCC Area—data management, statistics, etc.
6. User Information—user personal and PSC contact information
7. Admin/access control-administration tasks, user registration, etc.

A web-based GUI ensures data and structure flexibility, cross-platform independence and transparent Internet support. It was written primarily in PHP4 (<http://www.php.net>), complemented by Perl, JavaScript or Java. For secure, encrypted and automatic PSC-DCC data transfer, a combination of Unison (www.cis.upenn.edu/~bcpiercenison) and Secure Shell (SSH, www.ssh.com), was used.

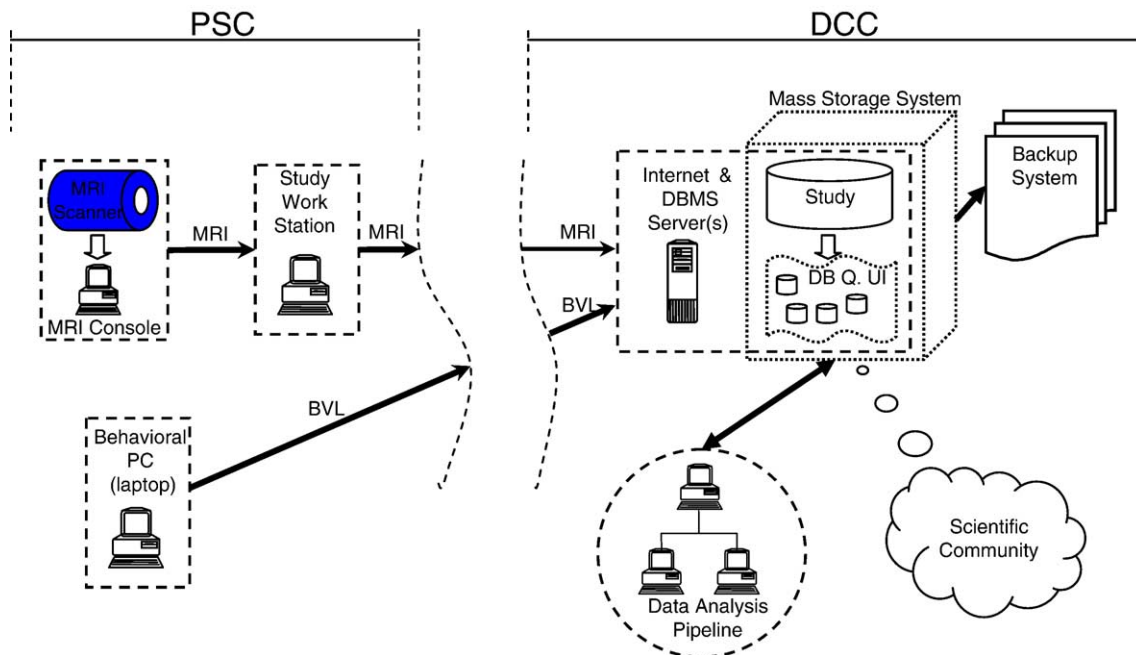


Fig. 4. Network connectivity between PSCs and DCC.

Data transfer procedures

The transfer mechanism (Fig. 4) used a study workstation at each PSC acting as data gateway between PSC and DCC. The study handled three types of data: (a) clinical/behavioral tests administered using paper-and-pencil test forms: data on these forms were entered into the database using a DCC-built web interface. Data entry for the paper-based tests used online pages that resemble those paper forms. Data entry typically resulted in computerized feedback to the PSCs (e.g., out-of-range entries, summary scores), (b) computerized tests (e.g., CANTAB) administered using the study laptop: data were automatically exported in a package to the DCC before undergoing the same quality control as the data arriving via the online interface, (c) MR scans. These were “pushed” from the MRI console to the workstation via DICOM transfer. At regular intervals, batches of MRI files were “pulled” from the workstation to the DCC using a “chron” job and an encrypted DICOM transfer protocol.

Data confidentiality and security

To ensure subject confidentiality and limit unauthorized access, all data were transferred and stored anonymously, identifiable only by two randomly assigned alphanumeric identifiers (PSC-ID and DCC-ID). Only coded subject information was stored at the DCC. All data transfer was encrypted with SSH and SSL. Finally, each user was assigned a user-name and password which determined the level of access (which sections of the database the user can access, what operations can be performed, whether the access is read-only or allows data modification). Five copies of all subject data exist, i.e., source data at PSC, copy on PSC workstation, archived CD copy at PSC, DCC database, archive CD copy at DCC.

Database quality control

Four levels of quality assurance were employed: (a) at data acquisition. Clinical/behavioral data were checked automatically for validity, type and range upon entry via on-screen forms. MRI scans were visually checked at the console, (b) at the PSC, before data transfer to DCC. Clinical/behavioral data were checked for entry completeness. Once all data for an instrument were entered, that instrument was marked as completed, disabling further editing. MRI data sets were qualitatively assessed at the workstation using 3D display software. A QC flag table was updated along with a comment list, providing a complete audit trail of data handling throughout the study, (c) at the DCC, upon receipt of the data at DCC. This verified the integrity and completeness of the received data, i.e., if the received files were correctly transmitted, whether the data set was complete and whether the correct acquisition parameters were used, (d) at the DCC, following integrity check. Clinical/behavioral data were verified against paper forms on a random subset of 1 in 3 candidates. MRI data were assessed both visually and using quantitative indices of image quality.

Two forms of calibration data were collected at each site: (a) The American College of Radiology (ACR) phantom: this phantom contains various compartments which provide information on intensity non-uniformity over a flat intensity field and geometric distortion over a grid pattern (collected approximately monthly), (b) the living phantom: one normal adult volunteer was scanned at all sites using the full MRI acquisition protocol. This database of real brain MRIs provided

information on inter-site variability in brain-related measures such as tissue contrast in raw MRI signal, tissue relaxation properties and derived morphological measurements (collected annually).

Image analysis

Structural MRI

Objective 1 MRI data were segmented using an automated image processing pipeline. However, this automated process has difficulty with Objective 2 data (age 0–4), due to variable tissue contrast and tight sulcal packing. Labor-intensive manual voxel labeling was performed for these cases using the DISPLAY tool. DISPLAY provides capabilities for (i) interactive 3D exploration of image volumes using simultaneous orthogonal planes and surface-rendered representations, (ii) manual labeling of image voxels, (iii) archival/recall of labeled 3D objects such as brain regions, tissue class maps, etc. and (iv) morphological operations such as dilate/erode/open/close. For the automated analysis of Objective 1 data, the methodologies detailed below were used for:

- Correction for image intensity non-uniformity
- Inter-packet registration for multislice T1W and T2W/PDW data
- Inter-modality (i.e., T2W and PDW to T1W) registration
- Identification of brain mask in native space
- Registration of T1W data to stereotaxic space
- Resampling of MRI data into stereotaxic space using tri-cubic resampling
- Identification of an intra-cranial cavity (ICC) mask to remove scalp, muscle, fat.

All image data for each subject were then resident in stereotaxic space, resampled on a 1 mm³ grid. 3D image segmentation then generated the following measures:

- Intra-cranial volume
- Total tissue (GM, WM and CSF) volumes
- Tissue density maps, using both linear and non-linear stereotaxic registration
- GM, WM and CSF volumes within individual lobes in both hemispheres
- Individual structure volumes (caudate, thalamus, superior temporal gyrus, etc.)
- Cortical surface thickness throughout cortex
- Regional (specific gyrus or lobe) cortical thickness means.

The main pipeline elements are described below.

Correction for 3D intensity non-uniformity—N3. N3 is a fully automated 3D technique for inhomogeneity correction. It maximizes the entropy of the intensity histogram to maximize its structure. The method is applicable to any pulse sequence, field strength and scanner (Sled et al., 1998).

Spatial normalization. Population variability in neuroanatomy was assessed using stereotaxic mapping strategies (Collins et al., 1994, 1995). Data were automatically mapped into

stereotaxic space using ANIMAL (see below) in two ways: (a) linear spatial normalization. a 9-parameter linear transformation such that anatomical variability among individual brains was captured as structure probability maps for each morphological entity. Voxels were anatomically labeled using three different segmentation approaches, and these maps were generated for (i) gray/white/CSF tissue classes (INSECT), (ii) major cortical gyri, cerebellum and deep subcortical nuclei (ANIMAL), (iii) cortical surfaces (CLASP). (b) Non-linear spatial normalization. High-dimensional non-linear warping was employed to map 3D native space into stereotaxic space such that neuroanatomical variability was captured in the resulting deformation fields (Worsley et al., 1996a,b,c).

Tissue classification—INSECT. INSECT (Intensity-Normalized Stereotaxic Environment for Classification of Tissues) takes pre-processed input volumes and generates tissue class (gray, white, CSF, lesion subtype) maps using an artificial neural network classifier (Zijdenbos et al., 2002; Cocosco et al., 2003).

Regional parcellation—ANIMAL. ANIMAL (Collins et al., 1994, 1995; Automated Non-linear Image Matching and Anatomical Labeling) uses a multi-scale approach to deform one MRI volume to match another, previously labeled, MRI volume. Anatomical labels are defined in the new volume by interpolation from the original labels, via the 3D deformation field. ANIMAL can be combined with INSECT to obtain finer detail in the regional segmentation (see Fig. 5).

Automatic surface parameterization—CLASP. CLASP (formerly MSD) is a fully automated iterative procedure for extracting and unfolding human cortex. It fits a 3D mesh model to a target cortical surface in the MRI volume. CLASP employs shape-preserving and surface intersection constraints to minimize a cost function which interpolates the deforming surface between the target surface and the current model surface. Two concentric linked surfaces map the gray/CSF and gray/white interfaces, allowing measurement of cortical thickness in 3D (Fig. 6, MacDonald et al., 2000; Kabani et al., 2001; Kim et al., 2005; Lerch and Evans, 2005).

Problems with surface extraction arise due to the mixing of signal from different tissue types in single MRI voxels, i.e., the partial volume effect (Tohka et al., 2004). These problems are particularly severe in pediatric brain MRI data where sulcal folds

are tightly packed, reducing the intra-sulcal CSF and preventing penetration of the deforming surface into the sulcus. Furthermore, the thin pediatric skull results in a close approach of the intense scalp signal to the brain parenchymal signal, causing additional partial volume problems. Finally, the poorer gray–white contrast in pediatric brain MRI presents further challenges for cortical surface extraction algorithms due to imperfect separation of tissue classes. Recently, a Laplacian-based enhancement has improved the surface detection for pediatric brain MRI (Kim et al., 2005; Lerch et al., 2005).

MR spectroscopy

Single voxel. The MRS data were analyzed with the LCModel package (Provencher, 1993, 2001) which reads raw ^1H MRS data files to produce fitted spectra with absolute metabolite concentrations. Each MRS voxel was co-registered with its tissue-segmented MRI and the voxel's volume % of gray matter, white matter and CSF determined. The MRS endpoints were CSF-corrected absolute levels of NAA, Cr and Cho.

MRSI. Data were also post-processed with the LCModel package as for single-voxel MRS. MRSI endpoints were CSF-corrected absolute levels of NAA, Glx, Cr, Cho and mI in left and right anterior cingulate gyri, prefrontal white matter, head of caudate nucleus, putamen, thalamus, insular cortex, parieto-occipital white matter, dorsolateral prefrontal cortex and mesial prefrontal cortex. Fig. 7 shows an example of the MRSI of the anterior cingulate.

Diffusion tensor imaging (DTI)

The DTI processing center (DPC) pipeline involves the following steps.

Sort DWIs and assign correct b-matrix to each image. Since b-matrix information was not available in the DICOM file-header, we used slice position, image number and series number to sort images.

Motion/distortion correction and registration. Patient motion and image distortion induced by eddy currents cause misregistration of the diffusion-weighted images (DWIs) from which the diffusion tensor was to be computed. We used the approach of Rohde et al. (2004), a combined mutual information-based registration technique and spatial transformation model, to correct

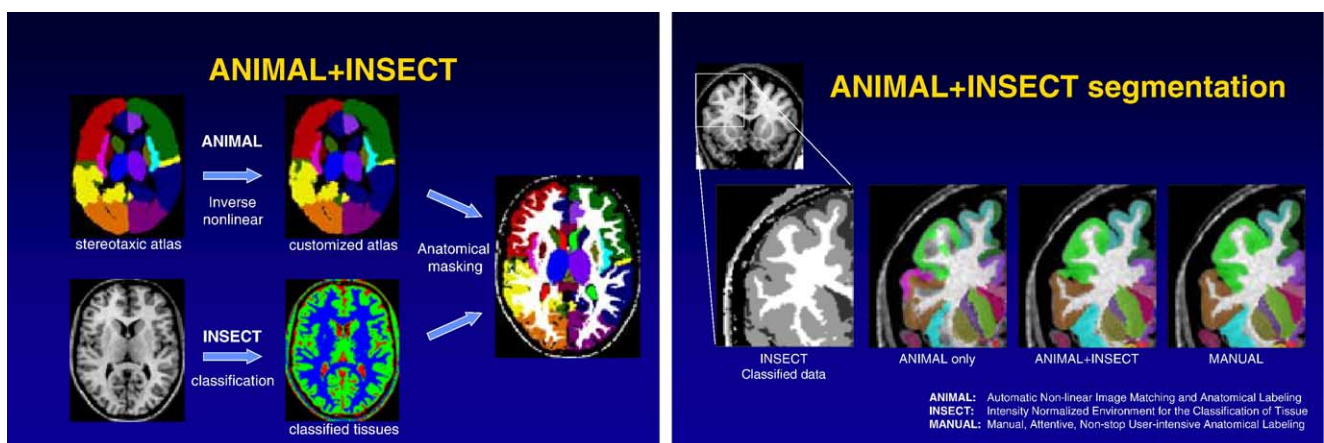


Fig. 5. Examples of automated regional parcellation obtained by combined INSECT and low-dimensional ANIMAL atlas warping.

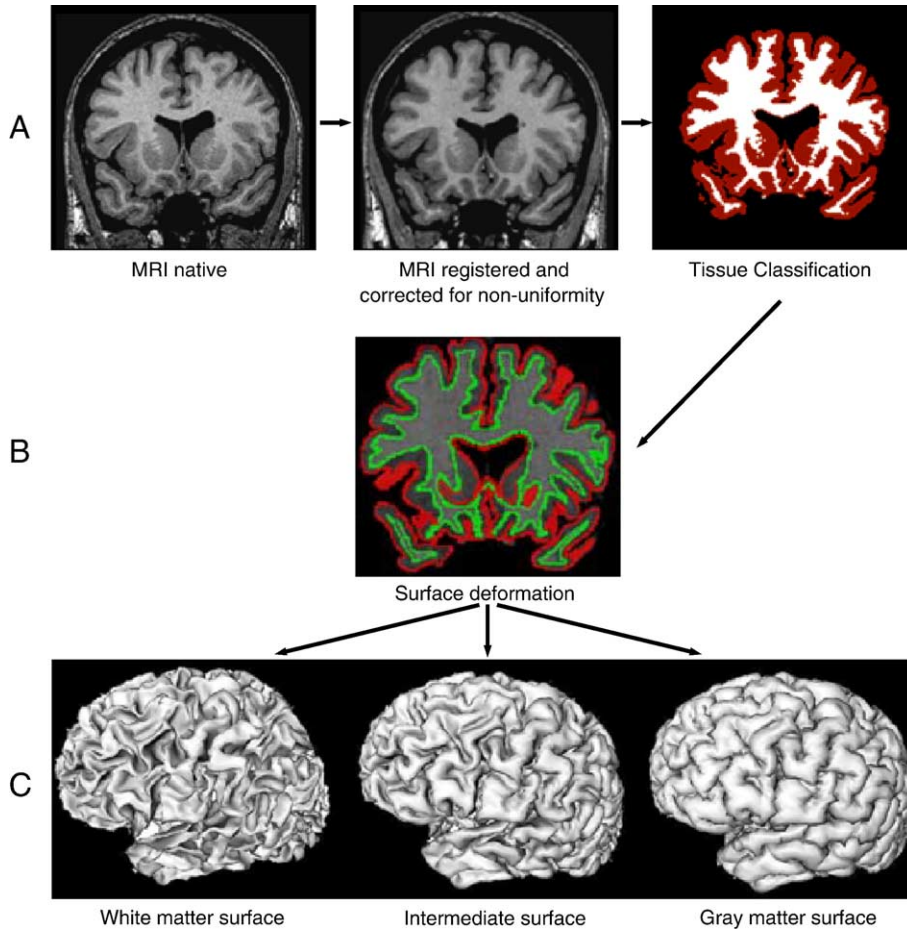


Fig. 6. Dual cortical surface extraction with CLASP.

simultaneously for both 3D rigid body motion and eddy-current-induced distortion. Images were corrected for EPI-induced distortions by registering them to the structural MRI for each subject. The signal amplitude of each DWI was corrected for size variations produced by the eddy current distortion correction. Images were resampled at 1 mm^3 resolution and the b-matrices recalculated in order to account for rotation applied during registration. All spatial transformations were concatenated into a single interpolation step.

Estimate the diffusion tensor: Diffusion tensor maps (Basser et al., 1994) were estimated by fitting the voxel intensity of the corrected DWIs as a function of their corresponding corrected b-matrix. Commonly used tensor fitting approaches, such as the linear least square regression method (Basser et al., 1994), assume signal variability in the DWIs to be affected only by white noise and to be spatially constant. However, spatially varying artifacts, e.g., from subject motion and cardiac pulsation, also contribute to signal variability. Neglecting such artifacts results in erroneous

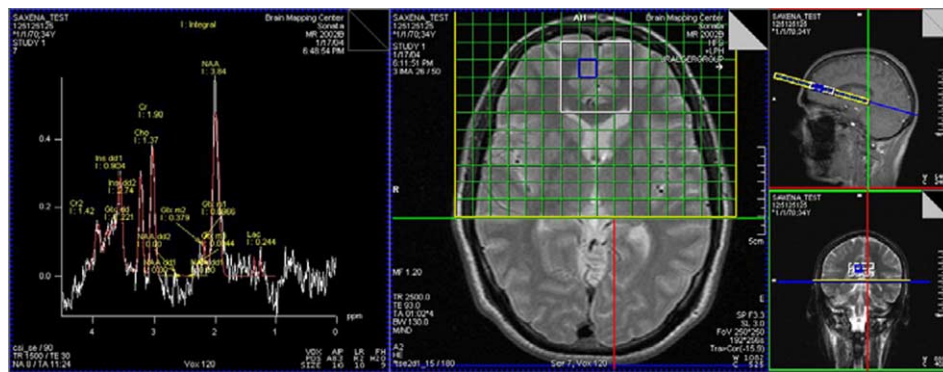


Fig. 7. Anterior cingulate MRSI. The MRSI slab (yellow box) was oriented parallel to the genu–splenic line, centered on the midplane of the basal ganglia. The PRESS volume (white box) was sized/positioned to sample the anterior cingulate gyri and lateral white matter without touching extra-brain tissue (lipid contamination) or crossing the horns of the ventricles. L: sample spectrum from selected voxel (blue).

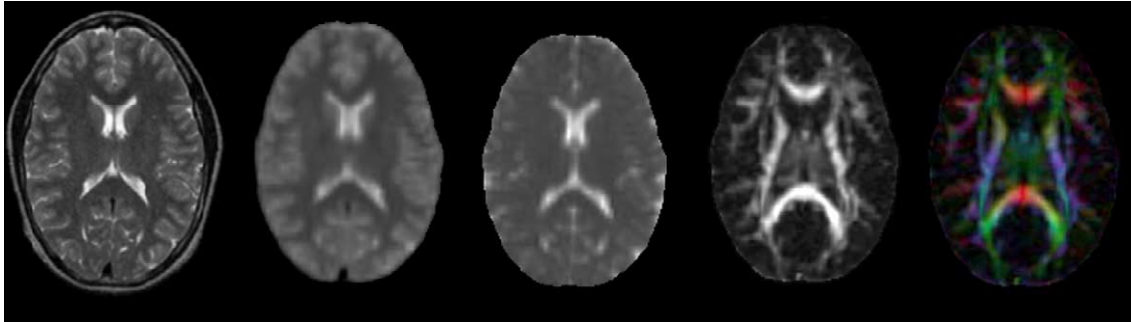


Fig. 8. DTI measures from L to R: reference structural T2-weighted image, amplitude image, trace (D) image, lattice index and color-coded maps of fiber orientation.

tensor values, so a robust non-linear tensor fitting algorithm based on iterative re-weighting was employed to identify and remove outliers (Chang et al., 2004).

Compute tensor-derived quantities. The following quantities were produced (Fig. 8):

- a) orientationally averaged diffusivity, i.e., Trace (D)/3 (Basser et al., 1994)
- b) fractional, relative and lattice anisotropy indices (Basser and Pierpaoli, 1996; Pierpaoli and Basser, 1996)
- c) eigenvalues of the diffusion tensor (Basser et al., 1994)
- d) color-coded maps of fiber orientation (Pajevic and Pierpaoli, 1999)
- e) Chi-square map of tensor fitting.

Produce stereotaxic maps of tensor-derived quantities. Stereotaxic DTI maps were obtained by scaling the images described above. Tensor re-orientation strategies (Alexander et al., 2001) were used to resample tensor quantities in stereotaxic space.

Statistical analysis

We investigated the relationship between (i) clinical/behavioral and demographic variables, (ii) neuroanatomical and demographic variables, and (iii) neuroanatomical and clinical/behavioral variables. The morphometric information (3D voxel-based tissue maps, regional volumetrics or vertex-based cortical surface metrics) was correlated with the clinical/behavioral data using both linear and non-linear models. The description below focuses on analysis of structural volume changes over time. However, these models can be equally well applied, with suitable correction for multiple comparisons, to the regression of voxel- or vertex-based structural data against any other demographic or clinical/behavioral variable.

Volume–time analysis

Regional growth was measured according to an accelerated longitudinal design (Harezlak et al., in press), a compromise between full longitudinal and cross-sectional designs. Longitudinal growth curves are fit by non-linear growth curve models (Jenss and Bayley, 1978; Preece and Baines, 1978) containing linear, quadratic and exponential terms to capture the curvilinear features of brain growth during key developmental epochs. Our models contain random child-specific effects that measure deviations from

population trends for individual children. We also fit semi-parametric models that are not restricted to the Jenss–Bailey model (Harezlak et al., in press) since evidence from an expanded version of the Giedd et al. (1999) study showed that the quadratic component of the Jenss–Bailey curves biases the fit at early and late ages. The semi-parametric regression models adapt to sharp changes in the data, e.g., growth spurts.

Proper treatment of non-linearities requires complex statistical methods, due to the presence of measurement error, additive rather than linear effects of subject-level covariates and patterned structures in temporal autocorrelations. Our modeling contains both conservative linear models and adaptive non-linear generalized additive models for situations where significant non-linearities exist (Hastie and Tibshirani, 1990).

Voxel-wise analysis

We are employing random field and generalized linear model for treatment of N-dimensional neuroimaging data. The general strategy (Worsley, 1994, 1995a,b; Worsley et al., 1996a; Cao, 1999; Cao and Worsley, 1999) has been applied to PET (Worsley et al., 1992, 1995, 1996b), anatomical MRI (Worsley et al., 1996c, 1999; Chung et al., 2001, 2003) and functional MRI (Worsley and Friston, 1995; Worsley et al., 2002; Liao et al., 2002). This forms the basis of voxel-wise analysis of MRI data and subsequent regression of morphological measures against independent clinical/behavioral measures (Paus et al., 1999, 2001; Giedd et al., 1999; Rapoport et al., 1999).

Results

Identification, screening and exclusions

(For a complete description of the screening procedures, please see website <http://www.bic.mni.mcgill.ca/nihpd/info>). A total of 35,429 introductory letters were mailed to families over an 18-month enrollment period, and 28,265 were successfully contacted. Approximately 8% of households contacted did not have a child in the age range of interest living in the area, and 13.5% spontaneously identified one or more exclusion factors prior to structured screening. Approximately 35% were not interested in participation. Large numbers of families were not pursued past an early contact as their family or child did not meet specific age, gender or other specified demographic variables to fill a remaining targeted recruitment cell. Overall, approximately 10% of contacted families ($N = 2861$) completed initial brief screening interviews, and 75.8%

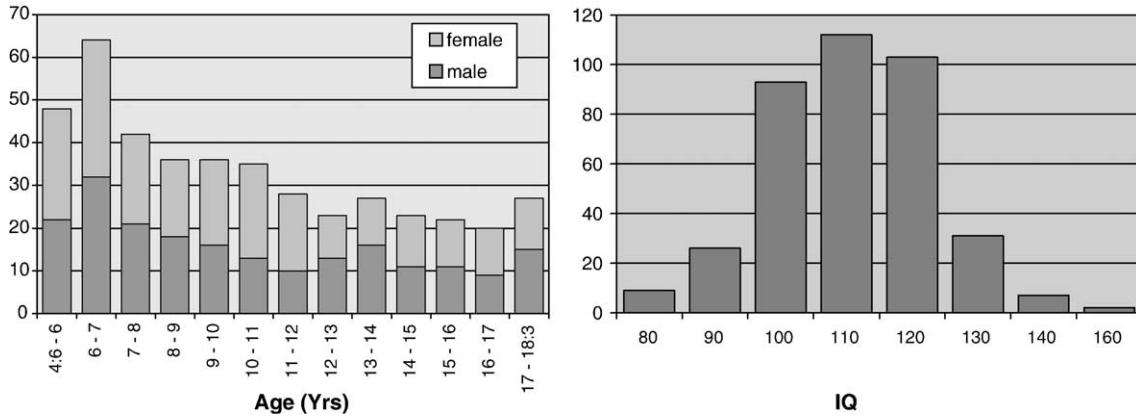


Fig. 9. Age Distribution (left) and Full Scale WASI IQ distribution (right) of Objective 1 sample ages 6 and older.

passed this stage and agreed to receive additional information and complete a parent-rated CBCL on the potential child of interest. 64.4% of these CBCLs were returned with an 85.2% passing rate. Further screening of these 1190 ($2861 \times 0.758 \times 0.644 \times 0.852$) families who completed initial screen steps and returned completed CBCLs yielded the 433 subjects who were enrolled for the full study. Thus, approximately 15.1% of screened families and 1.5% of contacted families were eventually enrolled as subjects in the full Objective I protocol.

Demographics of baseline sample

Age and gender. The Objective 1 cohort contains 433 subjects (224 F, 209 M). At each 1-year age interval, at least 20 subjects have been studied at baseline (Fig. 9). For children less than age 11, at least 30 subjects have been enrolled for each 1-year age range. The over-representation of younger children increases the cross-sectional and longitudinal data for these younger ages, when rapid developmental changes occur.

Ethnicity. The overall racial and ethnic distribution of the 433 enrolled subjects included 11% Black; 12% Hispanic; 1% Native Hawaiian or Native Pacific Islander; 2% American Indian or Alaskan Native; 2% Asian and 72% White. The U.S. Census provides data only for Black, Hispanic and White categories. The comparison of our sample demographics with these Census categories is shown in Table 8.

Socio-economic status (SES). Subjects were drawn from three SES categories (low, medium and high) based on family income after adjustment for cost of living in each PSC location and

family size. The U.S. Department of Housing and Urban Development (HUD) has established methods to compare family income levels based on regional costs of living and family size. Regionally specific HUD adjustment of raw family incomes is necessary given the diversity of U.S. regional economic and cost of living indices. Use of raw income numbers alone would underestimate the number of participating families living in low SES circumstances. The details of this HUD adjustment for SES are available at <http://www.bic.mni.mcgill.ca/nihpd/info>. These adjustments resulted in an increase in the proportion of “low-income” subjects across all racial/ethnic groups in the sample collected at our PSCs (see Table 8). When the HUD-based income categorizations of our sample are compared with the 2000 U.S. Census data, U.S. population subgroups defined according to income and race or ethnicity appear to be well represented in our sample (Chi-square $P = 0.27$; $df = 8$).

Clinical/behavioral data collection

As of May 2004, 6 months after completion of data collection, 100% data had been successfully transferred through the web interface to the DCC database. Since the database interface provides continuous feedback on data entry errors and summary scores, the overall error rate was low. In 154 subject profiles checked manually against source hard-copy results, each with approximately 1000 entries, a total of 734 input errors were detected, for an input error rate of 0.48%.

MRI

Of the 433 enrolled Objective 1 subjects, 426 completed their MRI studies for the baseline visit, of which 392 (92%) passed QC. 91 of these subjects had T1 fall-back scans, 116 had T2

Table 8
Total family SES categorization by race and ethnicity: overall U.S. family population (U.S. Census) vs. HUD-adjusted enrolled sample

Family SES categorization	Total		White ^a		Black ^a		Hispanic ^b	
	Sample	Census	Sample	Census	Sample	Census	Sample	Census
Low	22.9	34.8	13.9	23.9	5.8	5.8	3.2	5.0
Medium	41.6	37.4	31.9	29.9	3.9	3.8	5.8	3.6
High	35.5	27.8	30.4	24.6	1.7	1.8	3.4	1.4
Total	100.0	100.0	76.2	78.4	11.4	11.4	12.4	10.0

Source: U.S. Census Bureau, Statistical Abstract of the United States: 2000, Population p. 41.

^a Each race category excludes Hispanic ethnicity.

^b Hispanic of any race.

fall-back scans. The majority of the failures were due to subject motion. Subsequent packet-realignment processing of the raw MRI data at the DCC has now further reduced the number of Objective 1 MRI failures to 20 (4.7%). For Objective 2, a total of 193 studies have thus far been acquired from 72 subjects (all have multiple scans, some as many as 8 thus far). A total of 20 Objective 2 studies failed MRI QC (10.4%). As of January 2005, 619 MRI studies (426 + 193) had been successfully transferred to the DCC. For the DTI data, a total of 188 studies had been successfully completed from a planned total of 262 (71.8%).

Discussion

Structural MRI provides a means to determine healthy growth patterns for regional gray and white matter and various specific brain structures of interest. MRS provides a safe, noninvasive method for establishing a developmental profile of brain metabolites. DTI uses water diffusivity to probe structural and architectural changes occurring in brain tissue during development. The integration of information from these multiple modalities may generate a significant increase in the understanding of the structure, chemical composition and metabolic state of the healthy developing human brain. Such advances are required in order to better characterize brain development in children with a variety of brain disorders.

We have presented the NIH MRI Study of Normal Brain Development, summarizing the rationale, implementation and current data collection status of the project. The project has collected structural MRI, MRS, DTI and clinical/behavioral data in 500+ children aged 0–18 according to a uniform acquisition protocol. The protocol is a mixed cross-sectional/longitudinal design which will see repeated studies in each child over a 7-year period. We have successfully concluded the first cycle of data acquisition. A web-based database has been developed to store and analyze the study data. This database has also served as a feedback and status monitoring tool to assist in project management. All data have been successfully transferred to the Data Coordinating Center (DCC).

Sampling and recruitment

The full potential of imaging for elucidating healthy brain development in typically developing children can be realized only when longitudinal designs are combined with a sampling strategy designed to minimize bias, represent the diversity of the U.S. population and represent a wide range of normal variability in abilities. The design and implementation of the epidemiologic sampling plan used here meet these goals. The extensive clinical/behavioral data collected in the sample will allow brain maturation to be examined in relationship to pubertal status and to cognitive/neurobehavioral development.

The population-based sampling method reduced potential recruitment bias and allowed for characterization of potential bias in the sample based on available zip-code-based U.S. Census data. Families approached in the general population were receptive to considering participation in MRI studies of healthy brain development in their children. The sample enrolled and characterized is racially, ethnically, economically and educationally diverse, with the exception that there is a

smaller proportion of lower income Caucasians than would be expected based on total national demographic data.

As a truly normative database would need a substantially larger sample than the current resources allowed, we focused on a pediatric population with healthy brain development. Although the list of exclusion criteria is quite comprehensive, the sample characteristics span a wide range of healthy development and educational, economic, racial and ethnic background. While a large number of letters and initial contacts were initiated in order to ascertain the 433 subjects enrolled, many subjects who may have been otherwise eligible were not pursued because of the need to fill specific demographic cells.

Clinical/behavioral data

In the first cycle of data collection, a total of 9827 clinical/behavioral instruments were collected, 9029 from Objective 1 (Table 2) and 798 from Objective 2. Tight QC procedures have resulted in a rejection rate of <0.5%.

MRI

Quality control has demonstrated smaller than anticipated failure rates for structural MRI collection, on the order of 10% for both Objectives. Data analysis has begun for the structural MRI data. Illustrative results have been presented here; more complete analysis and discussion of results will appear in subsequent reports. Most of the early analysis was focused on structural MRI and morphological measures for correlation with demographic and clinical/behavioral variables.

Extensive diffusion tensor imaging (DTI) and MR spectroscopy (MRS MRSI) data have been collected. These are presently undergoing analysis at the DPC and SPC. Eventually, the T1 and T2 relaxometry files will be processed to provide voxel maps of estimated T1 and T2 values, hence providing insight into myelination of the developing brain. These maps will also be correlated with independent variables (age, clinical/behavioral measures) on a voxel-by-voxel basis.

Analyses are now under way to develop whole and regional brain developmental growth curves and to characterize the relationship between regional brain maturation and developmental changes in cognition and behavior. This study will provide for initial cross-sectional analyses at baseline and individual time point data but will also provide a large longitudinally sampled population to improve our power to detect and quantify regional growth curve trajectories. A number of investigators have already suggested the need for such larger longitudinal studies because of the impressive degree of variability that has been noted thus far in developmental imaging studies with children and adolescents. Such longitudinal studies have significantly increased power to detect longitudinal developmental change in populations with high heterogeneity, as compared with cross-sectional studies. In addition to providing a rich database of structural and chemical brain development, this study will characterize how neural development relates to medical status, neurological, cognitive, emotional and behavioral development.

We believe that the knowledge gained, together with the public release of this database in July 2006, will improve our understanding of pathophysiology and ultimately result in earlier, improved diagnostics and treatment for a broad range of diseases.

Acknowledgment

This project is supported by the National Institute of Child Health and Human Development (Contract N01-HD02-3343), the National Institute on Drug Abuse, the National Institute of Mental Health (Contract N01-MH9-0002), and the National Institute of Neurological Disorders and Stroke (Contracts N01-NS-9-2314, -2315, -2316, -2317, -2319 and -2320).

We wish to acknowledge the important contribution and remarkable spirit of John Haselgrove, Ph.D. (deceased) who contributed enormously to this project.

Appendix A. Brain Development Cooperative Group

The MRI Study of Normal Brain Development is a cooperative study performed by six pediatric study centers in collaboration with a Data Coordinating Center (DCC), a Clinical Coordinating Center (CCC), a Diffusion Tensor Processing Center (DPC), a Spectroscopy Processing Center (SPC) and staff of the National Institute of Child Health and Human Development (NICHD), the National Institute of Mental Health (NIMH), the National Institute for Drug Abuse (NIDA) and the National Institute for Neurological Diseases and Stroke (NINDS), Rockville, Maryland. Investigators from the six pediatric study centers are as follows: Children's Hospital Medical Center of Cincinnati, Principal Investigator William S. Ball, M.D., Co-Investigators Anna Weber Byars, Ph.D., Richard Strawsburg, M.D., Mark Schapiro, M.D., Wendy Bommer, R.N., April Carr, B.Sc., April German, B.A.; Children's Hospital Boston, Principal Investigator Michael J. Rivkin, M.D., Co-Investigators Deborah Haber, Ph.D., Robert Mulkern, Ph.D., Sridhar Vajapeyam, Ph.D., Abigail Chiverton, B.A., Peter Davis, S.B., Julie Koo, S.B., Jacki Marmor, M.A., Christine Mrakotsky, Ph.D., M.A., Richard Robertson, M.D., Gloria McAnulty, Ph.D., Sandra Kosta, B.A., M.A., Heidelise Als, Ph.D.; University of Texas Health Science Center at Houston, Principal Investigator Michael E. Brandt, Ph.D., Co-Principal Investigators Jack M. Fletcher, Ph.D., Larry A. Kramer, M.D., Co-Investigators Kathleen M. Hebert, Grace Yang, Vinod Aggarwal, M.D., Sushma V. Aggarwal; Washington University in St. Louis, Principal Investigators Kelly Botteron, M.D., Robert C. McKinstry, M.D., Ph.D., Co-Investigators William Warren, Tomoyuki Nishino, M.Sc., C. Robert Almlie, Ph.D., Richard Todd, Ph.D., M.D., John Constantino, M.D. Asif Moinuddin, M.D., Tina M. Day, B.A.; University of California Los Angeles (and SPC), Principal Investigator James T. McCracken, M.D., Co-Investigators Jennifer Levitt, M.D., Jeffrey Alger, Ph.D., Joseph O'Neil, Ph.D., Arthur Toga, Ph.D., Robert Asarnow, Ph.D., David Fadale, Laura Heinichen, Cedric Ireland; Children's Hospital of Philadelphia, Principal Investigator Dah-Jyuu Wang, Ph.D., Co-Principal Investigator Edward Moss, Ph.D., Co-Investigators Robert A. Zimmerman, M.D., Brooke Bintliff, B. Sc., Ruth Bradford, Janice Newman, M.B.A. The Principal Investigator of the Data Coordinating Center at McGill University is Alan Evans, Ph.D., Co-Investigators G. Bruce Pike, Ph.D., D. Louis Collins, Ph.D., Gabriel Leonard, Ph.D., Tomas Paus, M.D., Alex Zijdenbos, Ph.D., Rozalia Arnaoutelis, B.Sc, Lawrence Baer, M.Sc., Matt Charlet, Samir Das, B.Sc., Jonathan Harlap, Matthew Kitching, Denise Milovan, M.A., Dario Vins, B.Com., and at Georgetown University, Thomas Zeffiro, M.D., Ph.D. and John Van Meter, Ph.D. Nicholas Lange, Sc.D., Harvard University/McLean Hospital, is a statistical study design and data analysis Co-Investigator to the Data Coordinating Center.

The Principal Investigator of the Clinical Coordinating Center at Washington University is Kelly Botteron, M.D., Co-Investigators C. Robert Almlie Ph.D., Cheryl Rainey, B.Sc., Stan Henderson M.S., Tomoyuki Nishino, M.S., William Warren, Jennifer L. Edwards M.S.W., Diane Dubois R.N., Karla Smith, Tish Singer and Aaron A. Wilber, M.Sc. The Principal Investigator of the Diffusion Tensor Processing Center at the National Institutes of Health is Carlo Pierpaoli, MD, Ph.D., Co-Investigators Peter J. Basser, Ph.D., Lin-Ching Chang, Sc.D. and Gustavo Rohde. The Principal Collaborators at the National Institutes of Health are Lisa Freund, Ph.D. (NICHD), Judith Rumsey, Ph.D. (NIMH), Laurence Stanford, Ph.D. (NIDA), and from NINDS, Katrina Gwinn-Hardy, M.D. and Giovanna Spinella, M.D.

References

- Achenbach, T.M., 1997. Manual for the Young Adult Self-report and Young Adult Behavior Checklist. University of Vermont, Dept. of Psychiatry, Burlington, VT.
- Achenbach, T.M., 2001. Manual for the ASEBA School-Age Forms and Profiles (Child Behavior Checklist for Ages 6–18). ASBEA, Burlington, Vermont.
- Achenbach, T.M., Rescorla, L.A., 2000. Manual for the ASEBA Preschool Forms and Profiles (Child Behavior Checklist for Ages 1 1/2–5). ASBEA, Burlington, Vermont.
- Alexander, D.C., Pierpaoli, C., Basser, P.J., Gee, J.G., 2001. Spatial transformations of diffusion tensor magnetic resonance images. *IEEE Trans. Med. Imaging* 20, 1131–1139.
- Almlie, C.R., 1999. Measures of Hand Preference and Use Appropriate for Infants and Children. Washington University.
- Bartzokis, G., Bescos, M., Lu, P.H., Nuechterlein, K.H., Edwards, N., Mintz, J., 2001. Age-related changes in frontal and temporal lobe volumes in men: a magnetic resonance imaging study. *Arch. Gen. Psychiatry* 58 (5), 461–465.
- Basser, P.J., Pierpaoli, C., 1996. Microstructural and physiological features of tissues elucidated by quantitative-diffusion-tensor MR. *J. Magn. Res.*, 209–219.
- Basser, P.J., Mattiello, J., LeBihan, D., 1994. MR diffusion tensor spectroscopy and imaging. *Biophys. J.* 66, 259–267.
- Blanton, R.E., Levitt, J.G., Thompson, P.M., Narr, K.L., Capetillo-Cunliffe, L., Nobel, A., Singerman, J.D., McCracken, J.T., Toga, A.W., 2001. Mapping cortical asymmetry and complexity patterns in normal children. *Psychiatry Res.* 107 (1), 29–43.
- Blanton, R.E., Levitt, J.G., Peterson, J.R., Fadale, D., Sporty, M.L., Lee, M., To, D., Mormino, E.C., Thompson, P.M., McCracken, J.T., Toga, A.W., 2004. Gender differences in the left inferior frontal gyrus in normal children. *NeuroImage* 22 (2), 626–636.
- Blatter, D.D., Bigler, E.D., Gale, S.D., Johnson, S.C., Anderson, C.V., Burnett, B.M., Parker, N., Kurth, S., Horn, S.D., 1995. Quantitative volumetric analysis of brain MR: normative database spanning 5 decades of life. *Am. J. Neuroradiol.* 16 (2), 1199–1200.
- Cao, J., 1999. The size of the connected components of excursion sets of χ^2 , t and f fields. *Adv. Appl. Probab.* 31, 579–595.
- Cao, J., Worsley, K., 1999. The geometry of correlation fields, with an application to functional connectivity of the brain. *Ann. Appl. Probab.* 9, 1021–1057.
- Carskadon, M.A., Acebo, C., 1993. A self-administered rating scale for pubertal development. *J. Adolesc. Health* 14 (3), 190–195.
- Casey, B.J., Trainor, R., Giedd, J., Vauss, Y., Vaituzis, C.K., Hamburger, S., Kozuch, P., Rapoport, J.L., 1997. The role of the anterior cingulate in automatic and controlled processes: a developmental neuroanatomical study. *Dev. Psychobiol.* 30 (1), 61–69.
- Castellanos, F.X., Lee, P.P., Sharp, W., Jeffries, N.O., Greenstein, D.K., Clasen, L.S., Blumental, J.D., James, R.S., Ebens, C.L., Walter, J.M.,

- Zijdenbos, A., Evans, A.C., Giedd, J.N., Rapoport, J.L., 2002. Developmental trajectories of brain volume abnormalities in children and adolescents with attention-deficit/hyperactivity disorder. *J. Am. Med. Assoc.* 288 (14), 1740–1748.
- Caviness, V.S., Kennedy, D.N., Richelme, C., Rademacher, J., Filipek, P.A., 1996. The human brain age 7–11 years: a volumetric analysis based on magnetic resonance images. *Cereb. Cortex* 6 (5), 726–736.
- Caviness, V.S., Lange, N.T., Makris, N., Herbert, M.R., Kennedy, D.N., 1999. MRI-based brain volumetrics: emergence of a developmental brain science. *Brain Dev.* 21 (5), 289–295.
- CeNeS Limited, 1999. Cambridge Neuropsychological Test Automated Battery (CANTAB) for Windows Cambridge. CeNeS Limited, England.
- Chang, L.-C., Rohde, G.K., Jones, D.K., Bassler, P.J., Pierpaoli, C., 2004. RESTORE: robust estimation of tensors by outlier rejection. *Proc. ISMRM*, pp. 1223.
- Chung, M.K., Worsley, K.J., Paus, T., Cherif, C., Collins, D.L., Giedd, J.N., Rapoport, J.L., Evans, A.C., 2001. A unified statistical approach to deformation-based morphometry. *NeuroImage* 14 (3), 595–606.
- Chung, M.K., Worsley, K.J., Robbins, S., Paus, T., Taylor, J., Giedd, J.N., Rapoport, J.L., Evans, A.C., 2003. Deformation-based surface morphometry applied to gray matter deformation. *NeuroImage* 18, 198–213.
- Cloninger, C.R., Svrakic, D.M., Przybeck, T.R., 1993. A psychobiological model of temperament and character. *Arch. Gen. Psychiatry* 50 (12), 975–990.
- Cloninger, C.R., Przybeck, T.R., Svrakic, D.M., Wetzel, R.D., 1994. The Temperament and Character Inventory (TCI): A Guide to Its Development and Use. Center for Psychobiology of Personality, St. Louis.
- Cocosco, C.A., Zijdenbos, A.P., Evans, A.C., 2003. A fully automatic and robust MRI tissue classification method. *Med. Image Anal.* 7 (4), 513–527.
- Collins, D.L., Neelin, P., Peters, T.M., Evans, A.C., 1994. Automatic 3D registration of MR volumetric data in standardized Talairach space. *J. Comput. Assist. Tomogr.* 18 (2), 192–205.
- Collins, D.L., Holmes, C.J., Peters, T.M., Evans, A.C., 1995. Automatic 3D model-based neuroanatomical segmentation. *Hum. Brain Mapp.* 3, 190–208.
- Constantino, J.N., Cloninger, C.R., Clarke, A.R., Hashemi, B., Przybeck, T., 2002. Applications of the seven-factor model of personality to early childhood. *Psychiatry Res.* 15 (109), 229–243.
- Courchesne, E., Chisum, H.J., Townsend, J., Cowles, A., Covington, J., Egaas, B., Harwood, M., Hinds, S., Press, G.A., 2000. Normal brain development and aging: quantitative analysis at in vivo imaging in healthy volunteers. *Radiology* 216 (3), 672–682.
- DeBellis, M.D., Keshavan, M.S., Beers, S.R., Hall, J., Frustaci, K., Masalehdan, A., Noll, J., Boring, A.M., 2001. Sex differences in brain maturation during childhood and adolescence. *Cereb. Cortex* 11 (6), 552–557.
- Delis, D.C., Kaplan, E., Kramer, J.H., Ober, B.A., 1994. The California Verbal Learning Test-Children's Version. Psychological Corporation, San Antonio, Texas.
- Delis, D.C., Kaplan, E., Kramer, J.H., Ober, B.A., 2000. California Verbal Learning Test-II. Psychological Corporation, San Antonio, TX.
- Durston, S., Hulshoff Pol, H.E., Casey, B.J., Giedd, J.N., Buitelaar, J.K., van Engeland, H., 2001. Anatomical MRI of the developing human brain: what have we learned? *J. Am. Acad. Child Adolesc. Psychiatry* 40 (9), 1012–1020.
- Elliott, C.D., 1990a. DAS Administration and Scoring Manual. Psychological Corporation, Harcourt Brace and Company, San Antonio, TX.
- Elliott, C.D., 1990b. DAS Introductory and Technical Handbook. Psychological Corporation, Harcourt Brace and Company, San Antonio, TX.
- Elliott, C.D., 1990c. Differential Ability Scales. Psychological Corporation, Harcourt Brace and Company, San Antonio, TX.
- Filipek, P.A., Richelme, C., Kennedy, D.N., Caviness Jr., V.S., 1994. The young adult human brain: an MRI-based morphometric analysis. *Cereb. Cortex* 4 (4), 344–360.
- Gardner, R.A., Broman, M., 1979. The Purdue Pegboard: normative data on 1334 schoolchildren. *J. Clin. Psychol.* 8, 156–162.
- Giedd, J.N., Vaituzis, A.C., Hamburger, S.D., Lange, N., Rajapakse, J.C., Kaysen, D., Vauss, Y.C., Rapoport, J.L., 1996. Quantitative MRI of the temporal lobe, amygdala, and hippocampus in normal human development: ages 4–18 years. *J. Comp. Neurol.* 366 (2), 223–230.
- Giedd, J.N., Blumenthal, J., Jeffries, N.O., Castellanos, F.X., Liu, H., Zijdenbos, A., Paus, T., Evans, A.C., Rapoport, J.L., 1999. Brain development during childhood and adolescence: a longitudinal MRI study. *Nat. Neurosci.* 2 (10), 861–863.
- Gioia, G.A., Isquith, P.K., Guy, S.C., Kenworthy, L., 1996. Behavior Rating Inventory of Executive Function (BRIEF). Psychological Assessment Resources Inc., Odessa, FL.
- Gioia, G.A., Isquith, P.K., Guy, S.C., Kenworthy, L., 2000. Behavior rating inventory of executive function. *Child Neuropsychol.* 6 (3), 235–238.
- Gogtay, N., Giedd, J., Rapoport, J.L., 2002. Brain development in healthy, hyperactive, and psychotic children. *Arch. Neurol.* 59 (8), 1244–1248.
- Gogtay, N., Giedd, J.N., Lusk, L., Hayashi, K.M., Greenstein, D., Vaituzis, A.C., Nugent, T.F.R., Herman, D.H., Clasen, L.S., Toga, A.W., Rapoport, J.L., Thompson, P.M., 2004. Dynamic mapping of human cortical development during childhood through early adulthood. *Proc. Natl. Acad. Sci. U. S. A.* 101 (21), 8174–8179.
- Harezlak, J., Ryan, L., Giedd, J.N., Lange, N., 2005. Individual and population penalized regression splines for accelerated longitudinal designs. *Biometrics* (in press; early electronic publication at <http://www.blackwell-synergy.com/doi/abs/10.1111/j.1541-0420.2005.00376.x>).
- Haselgrove, J., Moore, J., Wang, Z., Traipe, E., Bilaniuk, L., 2000. A method for fast multislice T1 measurement: feasibility studies on phantoms, young children, and children with Canavan's disease. *J. Magn. Reson. Imaging* 11 (4), 360–367.
- Hastie, T., Tibshirani, R., 1990. Generalized Additive Models. Chapman and Hall, London.
- Initiative NSaBDG, 1992. Family Interview for Genetic Studies (FIGS). National Institute of Mental Health-Molecular Genetics Initiative.
- Jenss, R.M., Bayley, N., 1978. A mathematical method for studying the growth of a child. *Hum. Biol.* 9, 556–563.
- Jernigan, T.L., Tallal, P.A., 1990. Late childhood changes in brain morphology observable with MRI. *Dev. Med. Child Neurol.* 32 (5), 379–385.
- Jernigan, T.L., Trauner, D.A., Hesselink, J.R., Tallal, P.A., 1991. Maturation of human cerebrum observed in vivo during adolescence. *Brain* 114 (5), 2037–2049.
- Kabani, N., LeGoualher, G., MacDonald, D., Evans, A.C., 2001. Measurement of cortical thickness using an automated 3D algorithm: a validation study. *NeuroImage* 13 (2), 375–380.
- Kennedy, D.N., Lange, N., Makris, N., Bates, J., Meyer, J., Caviness Jr., V.S., 1998. Gyri of the human neocortex: an MRI-based analysis of volume and variance. *Cereb. Cortex* 8 (4), 372–384.
- Kennedy, D.N., Haselgrove, C., McInerney, S., 2003. MRI-based morphometry of typical and atypical brain development. *Ment. Retard. Dev. Disabil. Res. Rev.* 9 (3), 155–160.
- Kim, J.S., Singh, V., MacDonald, D., Lee, J.M., Kim, S.I., Evans, A.C., 2005. Automated 3D extraction and evaluation of the outer cortical surface using a Laplacian map and partial volume effect classification. *NeuroImage* 27, 210–221.
- Korkman, M., Kirk, U., Kemp, S., 1998. A Developmental Neuropsychological Assessment Manual. Psychological Corporation, Harcourt Brace and Co., San Antonio, TX.
- Lange, N.T., Giedd, J.N., Castellanos, F.X., Vaituzis, A.C., Rapoport, J.L., 1997. Variability of human brain structure size: ages 4–20 years. *Psychiatry Res.* 74 (1), 1–12.
- Lerch, J., Evans, A.C., 2005. Cortical thickness analysis examined through power analysis and a population simulation. *NeuroImage* 24 (1), 163–173.
- Lerch, J.P., Pruessner, J.C., Zijdenbos, A.P., Burger, K., Hampel, H., Teipel, S.J., Evans, A.C., 2005. Focal decline of cortical thickness in

- Alzheimer's disease identified by computational neuroanatomy. *Cereb. Cortex* 15 (7), 995–1001.
- Liao, C., Worsley, K., Poline, J.-B., Duncan, G.H., Evans, A.C., 2002. Estimating the delay of the hemodynamic response in fmri data. *NeuroImage* 16 (3), 593–606.
- Lucas, C.P., 2003. DISC Predictive Scales (DPS). Columbia University, New York, NY.
- Lucas, C.P., Zhang, H., Fisher, P.W., Shaffer, D., Regier, D.A., Narrow, W.E., Bourdon, K., Dulcan, M.K., Canino, G., Rubio-Stipec, M., Lahey, B.B., Friman, P., 2001. The DISC Predictive Scales (DPS): efficiently screening for diagnoses. *J. Am. Acad. Child Adolesc. Psych.* 40 (4), 443–449.
- Luciana, M., 2003. Practitioner review: computerized assessment of neuropsychological function in children: clinical and research applications of the Cambridge Neuropsychological Testing Automated Battery (CANTAB). *J. Child Psychol. Psychiatry Allied Discipl.* 44 (5), 649–663.
- Luciana, M., Nelson, C.A., 2002. Assessment of neuropsychological function through use of the Cambridge neuropsychological testing automated battery: performance in 4- to 12-year-old children. *Dev. Neuropsychol.* 22 (3), 595–624.
- MacDonald, D., Kabani, N., Avis, D., Evans, A.C., 2000. Automated extraction of inner and outer surfaces of cerebral cortex from MRI. *NeuroImage* 11, 564–574.
- Nellhaus, G., 1968. Head circumference from birth to eighteen years. Practical composite international and interracial graphs. *Pediatrics* 41 (1), 106–114.
- Pajevic, S., Pierpaoli, C., 1999. Color schemes to represent the orientation of anisotropic tissues from diffusion tensor data: application to white matter fiber tract mapping in the human brain. *Magn. Res. Med.* 42, 526–540.
- Paus, T., Zijdenbos, A., Worsley, K., Collins, D.L., Blumenthal, J., Rapoport, J., Evans, J.L., 1999. Structural maturation of neural pathways in children and adolescents: in vivo study. *Science* 283 (5409), 1908–1911.
- Paus, T., Collins, D.L., Evans, A.C., Leonard, G., Pike, B., Zijdenbos, A., 2001. Maturation of white matter in the human brain: a review of magnetic resonance studies. *Brain Res. Bull.* 54 (3), 255–266.
- Peterson, A.C., Crockett, L., Richards, M., Boxer, A., 1988. A self-report measure of pubertal status: reliability, validity, and initial norms. *J. Youth Adolesc.* 17, 117–133.
- Pfefferbaum, A., Mathalon, D.H., Sullivan, E.V., Rawles, J.M., Zipursky, R.B., Lim, K.O., 1994. A quantitative magnetic resonance imaging study of changes in brain morphology from infancy to late adulthood. *Arch. Neurol.* 51 (9), 374–387.
- Pierpaoli, C., Basser, P.J., 1996. Toward a quantitative assessment of diffusion anisotropy. *Magn. Res. Med.* 36, 893–906.
- Preece, M.A., Baines, M.J., 1978. A new family of mathematical models describing the human growth curve. *Ann. Hum. Biol.* 5 (1), 1–24.
- Provencher, S.W., 1993. Estimation of metabolite concentrations from localized in vivo proton NMR spectra. *Magn. Reson. Med.* 30, 672–679.
- Provencher, S.W., 2001. Automatic quantitation of localized in vivo ^1H spectra with LCModel. *NMR Biomed.* 14, 260–264.
- Rapoport, J.L., Giedd, J.N., Blumenthal, J., Hamburger, S., Jeffries, N., Fernandez, T., Nicolson, R., Bedwell, J., Lenane, M., Zijdenbos, A., Paus, T., Evans, A.C., 1999. Progressive cortical change during adolescence in childhood-onset schizophrenia: a longitudinal magnetic resonance imaging study. *Arch. Gen. Psychiatry* 56 (7), 649–654.
- Reiss, A.L., Abrams, M.T., Singer, H.S., Ross, J.L., Denckla, M.B., 1996. Brain development, gender and IQ in children. *Brain* 119 (5), 1763–1774.
- Robbins, T.W., James, M., Owen, A.M., Sahakian, B.J., Lawrence, A.D., McInnes, L., Rabbitt, P.M., 1998. A study of performance on tests from the CANTAB battery sensitive to frontal lobe dysfunction in a large sample of normal volunteers: implications for theories of executive functioning and cognitive aging. *Cambridge Neuropsychological Test Automated Battery. J. Int. Neuropsychol. Soc.* 4 (5), 474–490.
- Rohde, G.K., Barnett, A.S., Basser, P.J., Marengo, S., Pierpaoli, C., 2004. Comprehensive approach for correction of motion and distortion in diffusion-weighted MRI. *Magn. Res. Med.* 51, 103–114.
- Shaffer, D., Fisher, P., Lucas, C.P., Dulcan, M.K., Schwab-Stone, M.E., 2000. NIMH Diagnostic Interview Schedule for Children Version IV (NIMH DISC-IV): description, differences from previous versions, and reliability of some common diagnoses. *J. Am. Acad. Child Adolesc. Psych.* 39 (1), 28–38.
- Shaffer, D., Fischer, P., Lucas, C., Comer, J., 2003. Diagnostic Interview Schedule for Children (DISC-IV). Columbia University, New York, NY.
- Sled, J., Zijdenbos, A., Evans, A.C., 1998. A non-parametric method for automatic correction of intensity non-uniformity in MRI data. *IEEE Trans. Med. Imaging* 17, 87–97.
- Sowell, E.R., Thompson, P.M., Holmes, C.J., Batth, R., Jernigan, T.L., Toga, A.W., 1999. Localizing age-related changes in brain structure between childhood and adolescence using statistical parametric mapping. *NeuroImage* 9 (2 Pt. 1), 587–597.
- Sowell, E.R., Thompson, P.M., Rex, D., Kornsand, D., Tessner, K.D., Jernigan, T.L., Toga, A.W., 2002. Mapping sulcal pattern asymmetry and local cortical surface gray matter distribution in vivo: maturation in perisylvian cortices. *Cereb. Cortex* 12 (1), 17–26.
- Sowell, E.R., Peterson, B.S., Thompson, P.M., Welcome, S.E., Henkenius, A.L., Toga, A.W., 2003. Mapping cortical change across the human life span. *Neuroscience* 6 (3), 309–315.
- Sowell, E.R., Thompson, P.M., Leonard, C.M., Welcome, S.E., Kan, E., Toga, A.W., 2004a. Longitudinal mapping of cortical thickness and brain growth in normal children. *Neuroscience* 24 (38), 8223–8231.
- Sowell, E.R., Thompson, P.M., Toga, A.W., 2004b. Mapping changes in the human cortex throughout the span of life. *Neuroscientist* 10 (4), 372–392.
- Tanner, J.M., 1962. Growth at Adolescence. Blackwell Scientific Publications, Oxford, England.
- Tohka, J., Zijdenbos, A., Evans, A.C., 2004. Fast and robust parameter estimation for statistical partial volume models in brain MRI. *NeuroImage* 23 (1), 84–97.
- Wechsler, D., 1981. Wechsler Adult Intelligence Scale-Revised. Psychological Corporation, San Antonio, TX.
- Wechsler, D., 1991. Wechsler Intelligence Scale for Children., 3rd Ed. Psychological Corporation, Harcourt Brace and Company, San Antonio, TX.
- Wechsler, D., 1999. Wechsler Abbreviated Scale of Intelligence. Psychological Corporation, Harcourt Brace and Company, San Antonio, TX.
- Woodcock, R.W., McGrew, K.S., Mather, N., 2001. Woodcock–Johnson III Tests of Achievement. Riverside Publishing Itasca, Illinois.
- Worsley, K.J., 1994. Local maxima and the expected Euler characteristic of excursion sets of χ^2 , f and t fields. *Adv. Appl. Probab.* 26, 13–42.
- Worsley, K.J., 1995a. Boundary corrections for the expected Euler characteristic of excursion sets of random fields, with an application to astrophysics. *Adv. Appl. Probab.* 27, 943–959.
- Worsley, K.J., 1995b. Estimating the number of peaks in a random field using the Hadwiger characteristic of excursion sets, with applications to medical images. *Ann. Stat.* 23, 640–669.
- Worsley, K.J., Friston, K.J., 1995. Analysis of fMRI time-series revisited-again. *NeuroImage* 2, 173–181.
- Worsley, K.J., Evans, A.C., Marrett, S., Neelin, P., 1992. A three-dimensional statistical analysis for CBF activation studies in human brain. *J. Cereb. Blood Flow Metab.* 12, 900–918.
- Worsley, K.J., Poline, J.-B., Vandal, A.C., Friston, K.J., 1995. Tests for distributed, non-focal brain activations. *NeuroImage* 2, 183–194.
- Worsley, K.J., Marrett, S., Neelin, P., Vandal, A.C., Friston, K.J., Evans, A.C., 1996a. A unified statistical approach for determining signi-

- ficant signals in images of cerebral activation. *Hum. Brain Mapp.* 4 (1), 58–73.
- Worsley, K.J., Marrett, S., Neelin, P., Evans, A.C., 1996b. Searching scale space for activation in PET images. *Hum. Brain Mapp.* 4 (1), 74–90.
- Worsley, K.J., MacDonald, D., Cao, J., Shafie, K., Evans, A.C., 1996c. Statistical analysis of cortical surfaces. *NeuroImage* 3, S108.
- Worsley, K.J., Andermann, M., Koulis, T., MacDonald, D., Evans, A.C., 1999. Detecting changes in nonisotropic images. *Hum. Brain Mapp.* 8 (2–3), 98–101.
- Worsley, K.J., Liao, C., Aston, J., Petre, V., Duncan, G., Morales, F., Evans, A.C., 2002. A general statistical analysis for fmri data. *NeuroImage* 15, 1–15.
- Zijdenbos, A.P., Forghani, R., Evans, A.C., 2002. Automatic ‘pipeline’ analysis of 3D MRI data for clinical trials: application to multiple sclerosis. *IEEE Trans. Med. Imag.* 21 (10), 1280–1291.